# Potential capability of natural biosorbents: *Diplotaxis harra* and *Glebionis coronaria* L. on the removal efficiency of dyes from aqueous solutions

Hanane Tounsadi[a,b], Abderrahim Khalidi[a], Mohamed Abdennouri[b], Noureddine Barka[b,*]

[a]FSTM, Laboratoire d'Electrochimie, Chimie Physique, Bio-organique et Analytique (LECPBA), Université Hassan II Mohammedia Casablanca, BP 146, Mohammedia, Morocco, Tel. +212 645 20 85 64; email: hananetounsadi@gmail.com (H. Tounsadi), Tel. +212 661 64 09 93; email: khalidiabderrahim1@gmail.com (A. Khalidi)
[b]Laboratoire des Sciences des Matériaux, des Milieux et de la Modélisation (LS3 M), Univ Hassan 1, BP 145, Khouribga 25000 Morocco, Tel. +212 667 66 90 39, email: abdennourimohamed@yahoo.fr (M. Abdennouri), Tel. +212 661 66 66 22; Fax: +212 523 49 03 54; email: barkanoureddine@yahoo.fr (N. Barka)

## ABSTRACT

This study focuses on the use of natural biomaterials as a good alternative for dyes' removal from aqueous solutions. For this purpose, two local abundant plants *Diplotaxis harra* (*D. harra*) and *Glebionis coronaria* L. (*G. coronaria*) were chosen for the biosorption of methylene blue (MB) as a reference dye molecule due to its potential risk toward the environment and ecosystems, and malachite green (MG) representative of textile dyes. Biosorption experiments were carried out in batch mode as a function of solution pH, biosorbent dosage, contact time, initial dye concentration, and temperature. The experimental results show that the process is very rapid and the biosorption yield increases with an increase in the biosorbent dosage. Maximum biosorption capacity occurred at basic pH medium. The temperature doesn't have much influence on the biosorption yield. Kinetic data were analyzed using pseudo-first and pseudo-second kinetic orders. Equilibrium data were correlated to Langmuir, Freundlich, Temkin, and Dubinin–Radushkevich isotherm models. The best fit was obtained by Langmuir model with a maximum monolayer biosorption capacity of 185.59 and 64.37 mg/g in the case of *D. harra*, 258.76 and 117.32 mg/g in the case of *G. coronaria* L., respectively, for MB and MG.

*Keywords:* Biosorption; *Diplotaxis harra*; *Glebionis coronaria* L.; Kinetics; Equilibrium

## 1. Introduction

Organic dyes constitute one of the larger groups of pollutants in wastewater released from textile and other industries. The discharge of highly colored wastewater into the ecosystem involves environmental problems like esthetic pollution (even a small amount of dye is clearly apparent) and perturbation of aquatic life. Among $7 \times 10^5$ tons and approximately 10,000 different types of dyes and pigments produced worldwide annually, it is estimated that 1–15% of the dye is lost in the effluents during the dyeing process [1].

Most of these dyes are toxic, mutagenic, carcinogenic, and constitute serious pollution problems. From an environmental point of view, the removal of

*Corresponding author.

synthetic dyes is of great concern. Different processes have been employed for dye removal from colored effluents such as photocatalytic degradation [2], electrochemical oxidation [3], coagulation/filtration [4], ozonation [5], reverse osmosis [6], chemical precipitation [7], biologic treatments [8], and adsorption process [9]. Among all above-mentioned technologies, adsorption onto activated carbon has been considered the most efficient and applicable approaches in terms of simplicity and ease of operation [10,11]. However, the application of activated carbon has been limited because of its high cost and regeneration difficulties [12]. In order to improve the efficiency of the adsorption processes, it is necessary to develop cheaper and easily available adsorbents with high adsorption capacities. The use of natural biomaterials is a promising alternative due to their relative abundance. These waste materials have little or no economic value and often present disposal problem. Moreover, there is a need to valorize these low-cost byproducts. Recently, many industrial, agricultural, and forestry sources are used as biosorbents including *Scolymus hispanicus* L. [13], potato peel [14], cactus (*Opuntia ficus indica*) [15], tamarind seeds [16], *Daucus carota* [17], *fungi Poria cocos* [18], *Juglans regia* L. [19], and agricultural wastes [20].

The objective of the present study was to investigate the feasibility of *Diplotaxis harra* (*D. harra*) and *Glebionis coronaria* L. (*G. coronaria*) biomasses as biosorbents for dyes' removal from the aqueous solution. These plants are plentiful, easily available, and non-toxic; also they do not need a pre-treatment. Two types of dyes were chosen for this study, including methylene blue (MB) as a thiazine cationic dye commonly used as reference molecule for testing adsorption properties of materials, and malachite green (MG), a basic textile dye used for dyeing wool, leather, and cotton. Biosorption experiments were carried out as a function of contact time, biosorbent dosage, initial concentration of dyes, temperature, and solution pH. Equilibrium biosorption isotherms were modeled by Langmuir, Dubinin–Raduskevich, Temkin, and Freundlich models. The surface properties of biomasses were characterized by FTIR, BET specific surface area, and the point of zero charge (pH$_{PZC}$).

## 2. Materials and methods

### 2.1. Materials

All the chemicals used in this study were of analytical grade. MB (85%) was purchased from Panreac (Spain) and MG (100%) in its oxalate form was provided by Sigma–Aldrich (Germany). The chemical structures and physical properties of these dyes are shown in Table 1. NaOH was purchased from Merck (Germany), HNO$_3$ from Scharlau (Spain), and NaCl (99.5%) from Sigma–Aldrich (Germany).

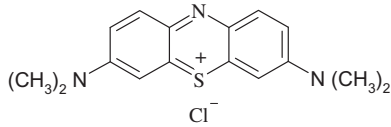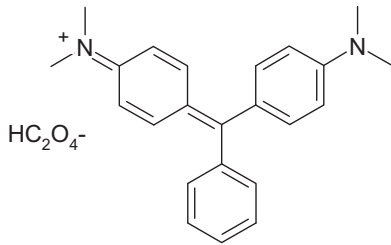### 2.2. Preparation and characterization of the biosorbents

*D. harra* and *G. coronaria* were collected from the region of Khouribga in Morocco. They were sun dried for 3 weeks, cut into small portions, and then powdered to particle sizes of 120 μm using a domestic mixer. The powder plants were dried in an oven at 70℃ for 24 h and stored in hermetic glass bottles. FTIR transmittance spectra of the biosorbents were recorded in the region of 4,000–400 cm$^{-1}$ using an ATR Miracle Diamante spectrometer by contacting a crystal (diamond) with the test sample without dilution in Ker matrix. Specific surface area was determined by N$_2$ adsorption according to the BET method using a Micromeritics model TRISTAR 3020 Instrument. The point of zero charge (pH$_{PZC}$) was determined by the pH drift method according to the method proposed by Noh and Schwarz [21]. The pH of NaCl aqueous solution (50 ml at 0.01 mol/L) was adjusted to successive initial values in the range of 2–12 by addition of HNO$_3$ and/or NaOH. Moreover, 0.05 g of each biosorbent was added in the solution and stirred for 6 h. The final pH was measured and plotted vs. the initial pH. The pH$_{PZC}$ was determined at the value for which pH$_{final}$ = pH$_{initial}$.

### 2.3. Biosorption studies

Stock solutions were prepared by dissolving desired weight of each dye in distilled water and necessary concentrations were obtained by dilution. Biosorption experiments were performed in a series of 50 mL beakers containing the desired weight of each biosorbent and 50 mL of the dye solution at desired concentration. These experiments were carried out at a constant agitation by varying pH of solution from 2 to 12, biosorbents dosage from 0.5 to 10 g/L, contact time from 5 to 180 min, initial dyes' concentration from 20 to 200 mg/L, and temperature from 10 to 50℃. The solution pH was adjusted by adding NaOH (0.1 N) or HNO$_3$ (0.1 N) and measured by a sensION + PH31 pH meter. The temperature was controlled using a thermostatically controlled incubator.

After each biosorption experiment completed, the solid phase was separated from the liquid phase by centrifugation at 3,000 rpm for 10 min. Each sample was diluted by distilled water and the residual concentrations were determined from UV–vis

Table 1
Chemical and physical properties of MB and MG

| Dye | Structure | Molecular weight (g/mol) | $\lambda_{max}$ (nm) |
|---|---|---|---|
| MB (Basic blue 9) | | 319.85 | 665 |
| MG (Basic green 4) | | 329.00 | 621 |

characteristics at maximum absorption wavelength of each dye (Table 1) using a TOMOS V-1100 UV–vis spectrophotometer.

The biosorption capacity and biosorption yield were calculated using the following equations:

$$q = \frac{(C_0 - C)}{R} \qquad (1)$$

$$\% \text{ Removal} = \frac{(C_0 - C)}{C_0} \times 100 \qquad (2)$$

where $q$ is the biosorbed quantity (mg/g), $C_0$ is the initial dye concentration (mg/L), $C$ is the dye concentration at a time $t$ (mg/L), and $R$ is the mass biosorbents per liter of solution (g/l).

## 3. Results and discussion

### 3.1. Characterization

The infrared spectra of *D. harra* and *G. coronaria* L. are illustrated in Fig. 1. The figure shows broad absorption band at 3,000–3,600 cm$^{-1}$ with a maximum at about 3,333.8 cm$^{-1}$ for *D. harra* and 3,334.7 cm$^{-1}$ for *G. coronaria* L. This band is characteristic of the stretching vibration of hydrogen bending of the hydroxyl group linked in cellulose, lignin, adsorbed water, and N–H Stretching [22]. The bands at 2,917 and 2,849.2 arise from aliphatic C–H stretching in an aromatic methoxyl group, in methyl and methylene groups of side chains. The $\nu(OH^-)$, $\nu(N–H)$, and $\nu(C–H)$ stretching is larger in the case of *D. harra* than of *G. coronaria* L. The small band at 1,700 cm$^{-1}$ is assigned to C=O stretching vibrations of ketones, aldehydes, lactones, or carboxyl groups. The band at 1,600–1,590 cm$^{-1}$ is due to O–H bending. The band
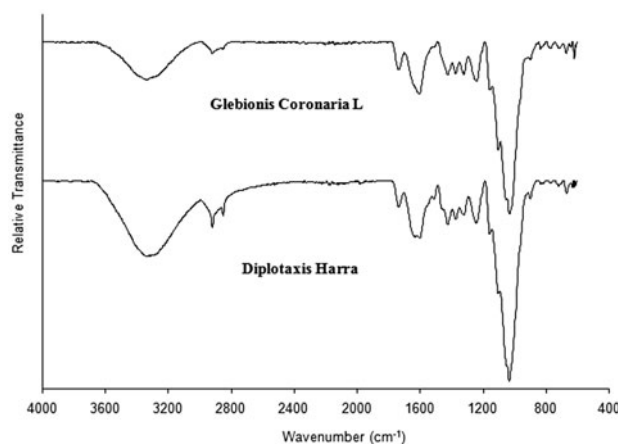


Fig. 1. FTIR spectra of *G. coronaria* L. and *D. harra* biosorbents.

1,423 cm$^{-1}$ is assigned to phenolic –OH and –C=O stretching of carboxylate. The band at 1,372 cm$^{-1}$ is characteristic of –COO groups. A very strong band at 1,032 cm$^{-1}$ could be assigned to =C–O–C, P=O stretching, or P–OH stretching. The bands at 898, 830, and 700 cm$^{-1}$ could be due to out-of-plane deformation mode of N-containing bioligands [23].

The specific surface area of the biosorbents was 1.612 and 1.741 m$^2$/g for *D. harra* and *G. coronaria* L., respectively. This small surface area suggested that these biosorbents do not have any defined holes on their morphology. The pH$_{PZC}$ were 6.29 for *D. harra* and 6.5 for *G. coronaria* L.

### 3.2. Effect of pH on the biosorption

Solution pH is one of the important process parameters that significantly influences the adsorption

of dyes on adsorbent. Fig. 2 shows the effect of pH on biosorption equilibrium of MG and MB onto *D. harra* and *G. coronaria* L. Significant biosorption onto both biosorbents occurred at a pH between 6 and 11 for MB, and between 5 and 12 for MG. Change in pH affects the biosorption process through dissociation of functional groups on the biosorbent surface active sites. The $pH_{PZC}$ were 6.29 for *D. harra* and 6.5 for *G. coronaria* L. These $pH_{PZC}$ values indicate that the biosorbents acquire a positive charge below a pH of 6.29 and 6.5, respectively, for *D. harra* and *G. coronaria* L. Above these values, the biosorbent surface become negatively charged [24]. Consequently, the ionic biosorbent–adsorbate interaction with cationic dyes (MB and MG) becomes progressively significant for pH higher than 6.29 and 6.5. A similar result was reported for the biosorption of Basic blue 41 by a silkworm pupa [25].

The quantities of MB adsorbed by *G. coronaria* L. are larger than those adsorbed by *D. harra*. This difference may be due to the nature of biosorbent–adsorbate interaction between the dye ions and functional groups of biosorbents.

### 3.3. Effect of biosorbent dosage

Data obtained from the experiments with varying biosorbent concentrations are presented in Fig. 3. The figure shows that increase in biosorbent dosage resulted in a sharp increase in the biosorption yield. The biosorption yield of MB increased from 67.42 to 83.58% and from 46.48 to 86.82% when the biosorbent dosage was increased from 0.25 to 1 g/L, respectively, for *D. harra* and *G. coronaria* L. For MG, the



Fig. 3. Effect of biosorbent dosage on biosorption of MB and MG by *D. harra* and *G. coronaria* L.: $C_0 = 100$ mg/L, contact time = 120 min, pH = initial pH, and $T = 25°C$.

biosorption yield increased from 21.61 to 89.19% and from 32.25 to 83.70% when the biosorbent dosage was increased from 0.25 to 4 g/L, respectively, for *D. harra* and *G. coronaria* L. The observed enhancement in biosorption yield with increasing biosorbent concentration could be due to an increase in the number of possible binding sites and surface area of the biosorbent [26]. A further increase in biomass concentration over 1 g/L for MB and 4 g/L for MG did not lead to a significant improvement in biosorption yield. This may be due to the decrease in driving force for mass transfer at low concentration of dyes in solution.

### 3.4. Biosorption kinetics

Biosorption rate gives an important information for designing batch biosorption systems. Information on the kinetics of solute uptake is required for selecting optimum operating conditions for full-scale batch process. Fig. 4 shows the plot of MB and MG biosorption vs. contact time. The biosorption was found to be rapid at the first period of the process and then the rate of biosorption becomes slower and then stagnates with the increase in contact time. The equilibrium time was 60 min for MB and 45 min for MG. In order to characterize the kinetics involved in the process of biosorption, pseudo-first-order and pseudo-second-order rate equations were proposed and the kinetic data were analyzed based on the regression coefficient ($r^2$) and the amount of dye biosorbed per unit weight of the biosorbent.

The first-order rate expression of Lagergren based on solid capacity is generally expressed as follows [27]:
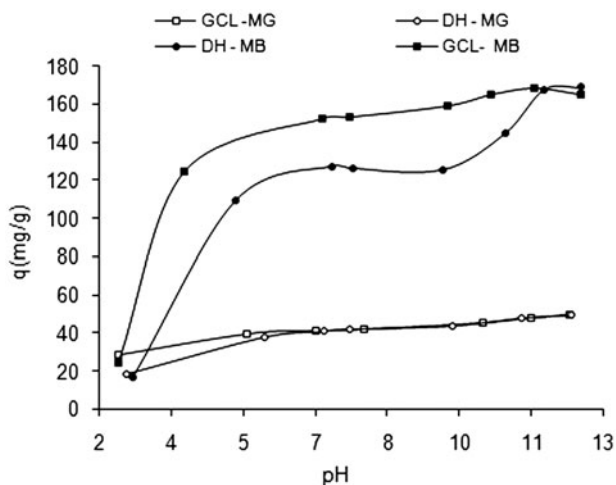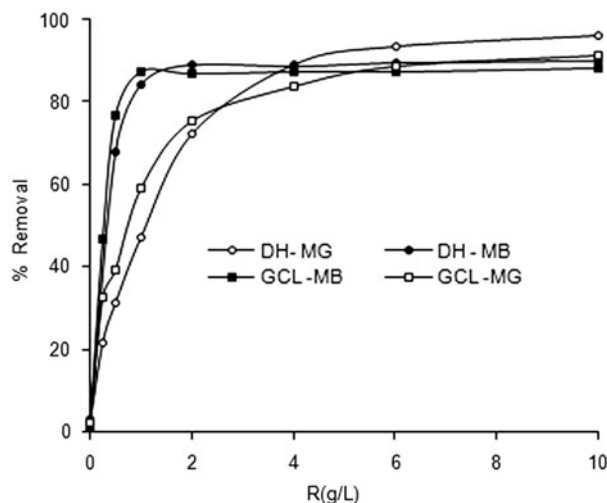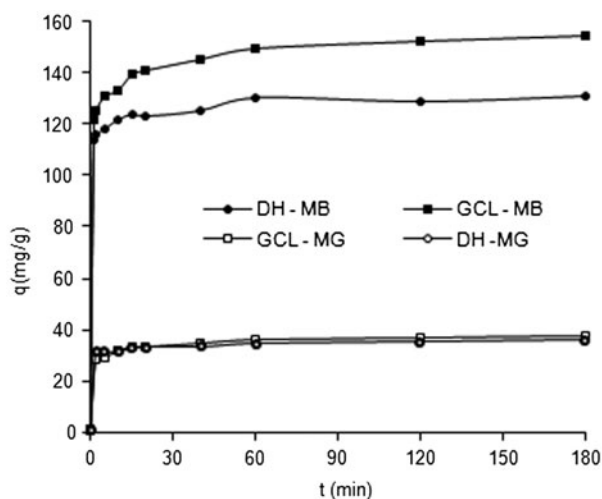


Fig. 2. Effect of pH on the biosorption of MB and MG onto *D. harra* and *G. coronaria* L.: $C_0 = 100$ mg/L, contact time = 120 min, $R = 0.5$ g/L, and $T = 25°C$.

Fig. 4. Kinetics of MB and MG biosorption by *D. harra* and *G. coronaria* L.: $C_0 = 100$ mg/L, $R = 0.5$ g/L, pH = initial solution pH, and $T = 25°C$.

$$q = q_e(1 - e^{-k_1 t}) \tag{3}$$

where $q_e$ and $q$ (both in mg/g) are, respectively, the amounts of dye biosorbed at equilibrium and at any time $t$ (min) and $k_1$ (1/min) is the rate constant of biosorption.

The pseudo-second-order model proposed by Ho and McKay [28] is based on the assumption that the biosorption follows second-order chemisorption. The pseudo-second-order model can be expressed as:

$$q = \frac{k_2 q_e^2 t}{1 + k_2 q_e t} \tag{4}$$

where $k_2$ (g/mg min) is the rate constant of pseudo-second-order biosorption.

The validity of each model was tested by judging the correlation coefficient, $r^2$, value and biosorption capacity ($q_{exp}$). Parameters of the pseudo-first-order and pseudo-second-order models were estimated with the aid of the non-linear regression using Origin 6.0 software. The experimental values of the amount of biosorption capacity and time were analyzed by non-linear curve fitting analysis in order to determine the models' parameters and the curves were reconstituted using the determined values. The obtained data and the correlation coefficients, $r^2$, are given in Table 2. The table shows that the values of correlation coefficient were closer to 1 in the case of pseudo-first-order than of pseudo-second-order model. Therefore, the calculated equilibrium values ($q_{cal}$) from

pseudo-first-order model were more compatible with the experimental equilibrium values ($q_{exp}$) than the others calculated from the pseudo-second-order model. This result suggests that the biosorption of MB and MG onto *D. harra* and *G. coronaria* L. could be better described by the pseudo-first-order model. This result provides that the biosorption capacity may be due to the higher driving force making fast transfer of MB and MG molecules to the surface of the biosorbent particles and the availability of the uncovered surface area and the remaining active sites on the adsorbent [29]. It results in a faster biosorption of MB and MG onto *D. harra* and *G. coronaria* L.

### 3.5. Effect of temperature

The variation in biosorbed quantities of MB and MG onto *D. harra* and *G. coronaria* L. as a function of solution temperature is shown in Fig. 5. It was observed that temperature has almost no effect on the biosorption of these dyes. Generally, the temperature has two major effects on the biosorption process. Increasing the temperature is known to increase the rate of the diffusion of molecules across the external boundary layer and the internal pores of the biosorbent particles, owing to the decrease in the viscosity of the solution. In addition, changing temperature will change the equilibrium capacity of the biosorbent for a particular adsorbate [30]. The observed trend may be due to the nature of the biosorbent particles which do not have any defined holes on their morphology.

### 3.6. Biosorption isotherms

The equilibrium biosorption capacity of *D. harra* and *G. coronaria* L. for MB and MG increased with a rise in dye initial concentration as shown in Fig. 6. The increase in biosorbed amounts with concentration is probably due to the high driving force for mass transfer. In fact, high concentration in solution implicates high amount of dye molecules fixed at the surface of the biosorbent. The isotherm was type L in Giles classification [31]. These types of isotherms are usually associated with ionic solute adsorption (e.g. metal cations and ionic dyes) with weak competition with the solvent molecules. To better understand the biosorption process, the obtained equilibrium biosorption data were analyzed by different isotherm models. An isotherm is characterized by some constants, the values of which express the surface properties and affinity of the biosorbent. An isotherm can also be used to analyze the biosorption capacity of biosorbents. In this study, Langmuir, Freundlich, Temkin,

Table 2
Pseudo-first-order and pseudo-second-order kinetic parameters for the biosorption of MB and MG by *D. harra* and *G. coronaria* L.

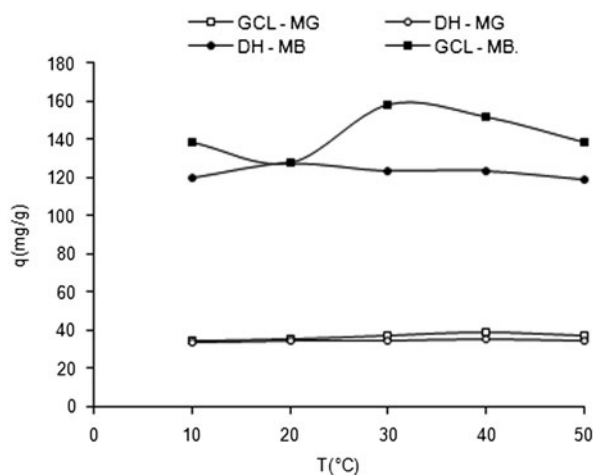| | Parameters | Pseudo-first-order | | Pseudo-second-order | |
|---|---|---|---|---|---|
| | | MB | MG | MB | MG |
| *D. harra* | $q_{exp}$ (mg/g) | 131.163 | 35.958 | 131.163 | 35.958 |
| | $q_{cal}$ (mg/g) | 124.713 | 33.633 | 123.368 | 33.359 |
| | $k$ (1/min) | 2.319 | 1.311 | 2.702 | 2.889 |
| | $r^2$ | 0.985 | 0.980 | 0.977 | 0.975 |
| *G. coronaria* L. | $q_{exp}$ (mg/g) | 154.186 | 37.625 | 154.186 | 37.625 |
| | $q_{cal}$ (mg/g) | 142.046 | 35.355 | 139.099 | 34.362 |
| | $k$ (g/mg min) | 1.756 | 0.790 | 3.149 | −1.913 |
| | $r^2$ | 0.961 | 0.949 | 0.938 | 0.887 |



Fig. 5. Effect of temperature on the biosorption of MB and MG onto *D. harra* and *G. coronaria* L.: $C_0 = 100$ mg/L, contact time = 120 min, pH = initial solution pH, and $R = 0.5$ g/l.

and Dubinin–Radushkevich models were selected to analyze the experimental equilibrium data.

### 3.6.1. Langmuir model

The Langmuir isotherm assumes that sorption comes from the monolayer coverage of adsorbate over a homogenous adsorbent surface [32]. This model supposes that sorption occurs on specific homogeneous sites within the adsorbent and all its sorption sites are energetically identical. The Langmuir isotherm can be written in the following form:

$$q_e = \frac{q_m K_L C_e}{1 + K_L C_e} \qquad (5)$$

where $q_m$ (mg/g) is the maximum monolayer biosorption capacity and $K_L$ (L/mg) is the Langmuir equilibrium constant related to the biosorption affinity. $C_e$ is the equilibrium concentration.

### 3.6.2. Freundlich model

The Freundlich isotherm is an empirical model of heterogeneous surface sorption with non-uniform distribution of heat sorption and affinities [33]. The form of the Freundlich equation can be stated as follows:

$$q_e = K_F C_e^{1/n} \qquad (6)$$

where $K_F$ (mg$^{1-1/n}$ g$^{-1}$ L$^{1/n}$) and $n$ are the Freundlich constants, $n$ is the heterogeneity factor related to biosorption affinity and $K_F$ is related to the biosorption capacity.

If the values of n are in the range of 1–10, it can be considered that the biosorption process indicates a favorable and slightly difficult biosorption. However, the biosorption is very insignificant when $n$ is lower than 1. Also, if the value of $n$ is equal to unity, the biosorption is linear; if the value is below unity, it can be deduced that biosorption process is chemical, if the value is above unity, adsorption is a favorable physical process.

### 3.6.3. Temkin model

Temkin isotherm model suggests a uniform distribution of binding energies and assumes the effects of the interaction of the adsorbate and the adsorbing species [34]. This isotherm assumes that the heat of adsorption of all the molecules in the layer would decrease linearly rather than logarithmically with
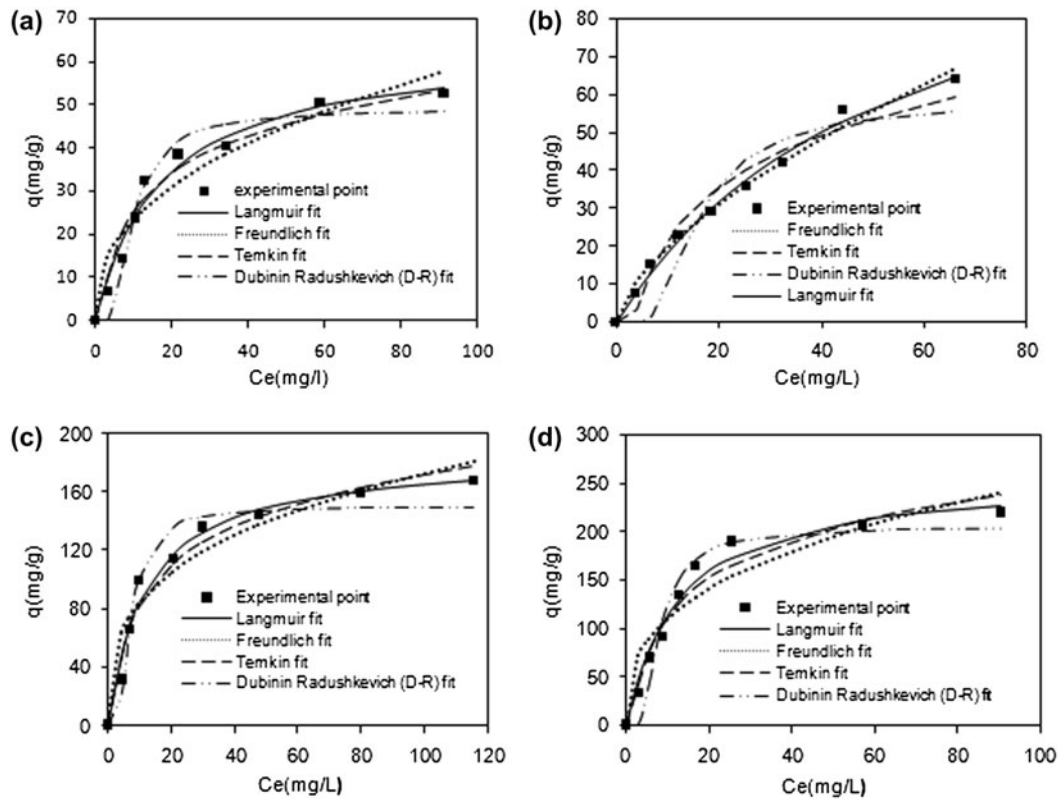
Fig. 6. Experimentals points and non-linear fited curves isotherms: MB onto *D. harra* (a), MB onto *G. coronaria* L. (b), MG onto *D. harra* (c), and MG onto *G. coronaria* L. (d).

coverage owing to adsorbate–biosorbent interactions. The Temkin isotherm has been expressed as:

$$q_e = B \ln(K_T C_e) \tag{7}$$

where $B = RT/b\,T$ (K) is the absolute temperature and $R$ is the universal gas constant (8.314 J/mol).

$B$ is the Temkin constant related to the heat of adsorption (kJ/mol) and $K_T$ is the empirical Temkin constant related to the equilibrium binding constant related to the maximum binding energy (L/mg).

### 3.6.4. Dubinin–Radushkevich model

The Dubinin–Radushkevich isotherm model does not assume a homogenous surface or constant sorption potential as other models. It can be noted that the Dubinin–Radushkevich isotherm is more general than the Langmuir model [35]. The Dubinin–Radushkevich isotherm is expressed by the following equation:

$$q_e = q_m \exp(-B\varepsilon^2) \tag{8}$$

$$\varepsilon^2 = RT \, \ln\left(1 + \frac{1}{C_e}\right)$$

where $B$ is a constant related to the adsorption energy, $q_{max}$ is the theoretical saturation capacity, and is the Polanyi potential.

The calculated isotherm parameters for each model and correlation coefficients estimated by non-linear regressive method are summarized in Table 3. The table indicates that the best fit of experimental data was obtained with the Langmuir model. The values of $r^2 \geq 0.9765$ accused the applicability of the Langmuir model for dyes' biosorption onto the *D. harra* and *G. coronaria* L. The maximum Langmuir monolayer biosorption capacities were 185.59 and 258.76 mg/g for MB and 64.37 and 106.44 mg/g in the case of MG, respectively, for *D. harra* and *G. coronaria* L.

For the Freundlich model, the correlation coefficients are lower. Then this model did not provide any information about the saturation biosorption capacity such as the Langmuir model. Only the biosorption of MG onto *G. coronaria* L. showed significance, where $r^2 = 0.98$. The values of $n > 1$ indicated favorable

Table 3
Isotherm constant parameters and correlation coefficients calculated for the biosorption of MB and MG onto *D. harra* and *G. coronaria* L.

| Isotherms | Parameters | *D. harra* | | *G. coronaria* L. | |
|---|---|---|---|---|---|
| | | MB | MG | MB | MG |
| Langmuir | $q_m$ (mg/g) | 185.59 | 64.37 | 258.76 | 117.32 |
| | $K_L$ (L/mg) | 0.08 | 0.05 | 0.08 | 0.01 |
| | $r^2$ | 0.976 | 0.975 | 0.975 | 0.992 |
| Freundlich | $n$ | 3.16 | 2.44 | 2.82 | 1.54 |
| | $K_F$ (mg$^{1-1/n}$ g$^{-1}$ L$^{1/n}$) | 40.60 | 9.13 | 49.24 | 4.48 |
| | $r^2$ | 0.924 | 0.926 | 0.89 | 0.989 |
| Temkin | $B$ (kJ/mol) | 63.48 | 171.67 | 43.40 | 125.11 |
| | $K_T$ (L/mg). | 0.83 | 0.51 | 0.72 | 0.30 |
| | $r^2$ | 0.940 | 0.963 | 0.940 | 0.950 |
| Dubinin–Radushkevich | $q_{max}$ (mg/g) | 150.51 | 48.89 | 205.02 | 58.23 |
| | $B$ (kJ/mol) | 7.06 E-6 | 0.00001 | 8.52 E-6 | 0.00003 |
| | $r^2$ | 0.933 | 0.936 | 0.928 | 0.811 |

biosorption under experimental conditions of both the dyes' sorption onto both the biosorbents. The Temkin model provides a calculation about equilibrium binding constant corresponding to the maximum binding energy, $K_T$. This model presents correlation coefficient $r^2 > 0.9405$ for both the dyes. On the other side, it is clear that the Dubinin–Radushkevich model is less suitable for fitting the experimental isotherm curves, as indicated by the lower values of $r^2$ and the greater value of $q_m$. Therefore, it is observed in Fig. 6 that the fitted curves from the Langmuir model were closer to the experimental data under experimental conditions. Moreover, the Langmuir isotherm was the most adapted to describe this sorption for both the dyes onto both the biosorbents. Comparing the optimization data between the four models, it is obvious that the Langmuir model is the most suitable to fit the biosorption isotherms, although Temkin model is more adapted than Freundlich and Dubinin–Radushkevich models. The higher MB sorption in both the materials could be due to the nature of the interaction between each adsorbate and sorbent. The *G. coronaria* L. biosorption capacity is better than the sorption of *D. harra*, which could be due to the larger specific surface of *G. coronaria* L.

Maximum biosorption capacity obtained from the biosorption of MB and MG onto *D. harra* and *G. coronaria* L. was compared to the previous records of various low-cost biosorptions as summarized in Table 4. It can be observed that experimental data of the present study were found to be higher than those of the most corresponding biosorbents in the literature. The result from this study can be due to the nature of functional groups present in the surface of *D. harra* and *G. coronaria* L.

Table 4
Comparison of maximum biosorption capacity of *D. harra* and *G. coronaria* L. for MB and MG with corresponding low-cost biosorbents

| Biosorbent | $q$ (mg/g) MB | $q$ (mg/g) MG | Refs. |
|---|---|---|---|
| Rice husk | 40.59 | 7.40 | [36,37] |
| Cotton waste | 277.77 | – | [38] |
| Papaya seeds | 555.55 | – | [39] |
| Coconut husk | 99.00 | – | [40] |
| Coffee husks | 90.10 | – | [41] |
| Teak wood bark | 84.00 | – | [42] |
| Raw date pits | 80.30 | – | [43] |
| Banana peel | 20.80 | – | [44] |
| Cereal chaff | 20.30 | – | [45] |
| Lemon peel | – | 51.73 | [46] |
| Ginger waste | – | 84.03 | [47] |
| De-oiled soya | – | 20.44 | [48] |
| Maize cob | – | 80.64 | [49] |
| Sea shell powder | – | 42.33 | [50] |
| *Luffa cylindrica* | – | 29.40 | [51] |
| *D. harra* | 185.59 | 64.37 | This study |
| *G. coronaria* L. | 258.76 | 117.32 | This study |

## 4. Conclusion

In this work, *D. harra* and *G. coronaria* L. were used as low-cost natural biosorbents for the removal of MB and MG from aqueous solutions. The ability of these biosorbents was investigated using various biosorption conditions. It was found that the sorption process was very rapid, the equilibrium time was obtained at 60 min for MB and 45 min for MG. The biosorption yield increases with the increase of biosorbent dosage

with an optimum at 0.5 g/L. The optimum biosorption was obtained at basic pH medium. The equilibrium uptake of these dyes was increased by the increasing of the initial concentration. The biosorption kinetic data fitted well to the pseudo-first-order kinetic model. The biosorption equilibrium data were best fitted by the Langmuir isotherm model under these optimum conditions. The temperature does not have much influence on the biosorption performance. Therefore, the biosorption was carried out at ambient pH which was higher than pHpzc. We can also summarize that 0.5 g/L is the optimum dosage of *D. harra* and *G. coronaria* L. for the removal of MB and MG under the experimental conditions. Finally, it can be concluded that *D. harra* and *G. coronaria* L. could be efficient biosorbents for the removal of dyes from aqueous solutions, also they can be used for the production of activated carbon using for the same reason.

## References

[1] H. Zollinger, Color Chemistry: Synthesis, Properties and Applications of Organic Dyes and Pigments, VCH, New York, NY, 1991.

[2] N. Barka, S. Qourzal, A. Assabbane, A. Nounah, Y. Ait-Ichou, Photocatalytic degradation of patent blue V by supported TiO$_2$: Kinetics, mineralization, and reaction pathway, Chem. Eng. Commun. 198 (2011) 1233–1243.

[3] P. Kariyajjanavar, J. Narayana, Y. Arthoba Nayaka, Degradation of textile dye C.I. Vat Black 27 by electrochemical method by using carbon electrodes, J. Environ. Chem. Eng. 1(4) (2013) 975–980.

[4] A.Y. Zahrim, N. Hilal, Treatment of highly concentrated dye solution by coagulation/flocculation–sand filtration and nanofiltration, Water Res. Ind. 3 (2013) 23–34.

[5] F. Gholami-Borujeni, K. Naddafi, F. Nejatzade-Barandozi, Application of catalytic ozonation in treatment of dye from aquatic solutions, Desalin. Water Treat. 51 (2013) 6545–6551.

[6] A. Aouni, C. Fersi, M. Dhahbi, Performance evaluation of direct nanofiltration process to fouling by treating rinsing-bath effluents for water reuse, Desalin. Water Treat. 52 (2014) 1770–1785.

[7] C.S. Gabriela, S.T.C. Virginia, M.F. Angela, C.P. Nathalia, P.P. Paulo Renato, L.L. Jorge, A facile synthesis of Mn$_3$O$_4$/Fe$_3$O$_4$ superparamagnetic nanocomposites by chemical precipitation: Characterization and application in dye degradation, Mater. Res. Bull. 49 (2014) 544–551.

[8] V.J. Leebana, H. Santhanam, K. Geetha, S.A. Raj, Biodegradation of direct golden yellow, a textile dye by *Pseudomonas putida*, Desalin. Water Treat. 39 (2014) 1–9.

[9] R. Elmoubarki, F.Z. Mahjoubi, H. Tounsadi, J. Moustadraf, M. Abdennouri, A. Zouhri, A. El Albani, N. Barka, Adsorption of textile dyes on raw and decanted Moroccan clays: Kinetics, equilibrium and thermodynamics, Water Res. Ind. 9 (2015) 16–29.

[10] K. Elmerzouki, A. Khalidi, R. Abdelhedi, I. Bimaghra, P. Taxil, B. Lafage, A. Savall, Removal of Cr(VI) and Pb(II) from aqueous solution by activated sawdust, Phys. Chem. News 64 (2012) 76–86.

[11] N. Barka, A. Assabbane, Y. Aît, A. Ichou, A. Nounah, Decantamination of textile wastewater by powdered activated carbon, J. Appl. Sci. 63 (2006) 692–695.

[12] M. Arulkumar, P. Sathishkumar, T. Palvannan, Optimization of Orange G dye adsorption by activated carbon of *Thespesia populnea* pods using response surface methodology, J. Hazard. Mater. 186 (2011) 827–834.

[13] N. Barka, M. Abdennouri, M. EL Makhfouk, Removal of Methylene Blue and Eriochrome Black T from aqueous solutions by biosorption on *Scolymus hispanicus* L.: Kinetics, equilibrium and thermodynamics, J. Taiwan Inst. Chem. Eng. 42 (2011) 320–326.

[14] E. Hoseinzadeh, M.-R. Samarghandi, G. McKay, N. Rahimi, J. Jafari, Removal of acid dyes from aqueous solution using potato peel waste biomass: A kinetic and equilibrium study, Desalin. Water Treat. 52 (2014) 4999–5006.

[15] N. Barka, K. Ouzaouit, M. Abdennouri, M. El Makhfouk, Dried prickly pear cactus (*Opuntia ficus indica*) cladodes as a low-cost and eco-friendly biosorbent for dyes removal from aqueous solutions, J. Taiwan Inst. Chem. Eng. 44 (2013) 52–60.

[16] P. Senthil Kumar, R. Sivaranjanee, U. Vinothini, M. Raghavi, K. Rajasekar, K. Ramakrishnan, Adsorption of dye onto raw and surface modified tamarind seeds: Isotherms, process design, kinetics and mechanism, Desalin. Water Treat. 52 (2014) 2620–2633.

[17] A.K. Kushwaha, N. Gupta, M.C. Chattopadhyaya, Removal of cationic methylene blue and malachite green dyes from aqueous solution by waste materials of *Daucus carota*, J. Saudi Chem. Soc. 18(3) (2014) 200–207.

[18] H. Zhang, Y. Tang, X.A. Liu, Z.G. Ke, X. Su, D.Q. Cai, X.Q. Wang, Y.D. Liu, Q. Huang, Z.L. Yu, Improved adsorptive capacity of pine wood decayed by *fungi Poria cocos* for removal of malachite green from aqueous solutions, Desalination 274 (2011) 97–104.

[19] F. Deniz, Potential use of shell biomass (*Juglans regia* L.) for dye removal: Relationships between kinetic pseudo-second-order model parameters and biosorption efficiency, Desalin. Water Treat. 52 (2014) 219–226.

[20] S. Rangabhashiyam, N. Anu, N. Selvaraju, Sequestration of dye from textile industry wastewater using agricultural waste products as adsorbents, J. Environ. Chem. Eng. 1(4) (2013) 629–641.

[21] J.S. Noh, J.A. Schwarz, Estimation of the point of zero charge of simple oxides by mass titration, J. Colloid Interface Sci. 130 (1989) 157–164.

[22] M.R.H. Mas Haris, K. Sathasivam, The removal of methyl red from aqueous solution using banana pseudostem fibers, J. Am. Appl. Sci. 6 (2009) 1690–1700.

[23] N. Barka, M. Abdennouri, M. El Makhfouk, S. Qourzal, Biosorption characteristics of cadmium and lead onto eco-friendly dried cactus (*Opuntia ficus indica*) cladodes, J. Environ. Chem. Eng. 1 (2013) 144–149.

[24] N. Barka, S. Qourzal, A. Assabbane, A. Nounah, Y. Ait-Ichou, Removal of Reactive Yellow 84 from aqueous solutions by adsorption onto hydroxyapatite, J. Saudi Chem. Soc. 15 (2011) 263–267.

[25] B. Noroozi, G.A. Sorial, H. Bahrami, M. Arami, Equilibrium and kinetic adsorption study of a cationic dye by a natural adsorbent—Silkworm pupa, J. Hazard. Mater. 139 (2007) 167–174.

[26] I. Bakas, K. Elatmani, S. Qourzal, N. Barka, A. Assabbane, Y. Ait-Ichou, A comparative adsorption for the removal of p-cresol from aqueous solution onto granular activated charcoal and granular activated alumina, J. Mater. Environ. Sci. 5(3) (2014) 675–682.

[27] S. Lagergren, About the theorie of so-called adsorption of soluble substance, Kungliga Svenska Vetenskapsakademiens Handlingar 24 (1898) 1–39.

[28] Y.S. Ho, G. Mckay, The kinetics of sorption of basic dyes from aqueous solution by sphagnum moss peat, Can. J. Chem. Eng. 76 (1998) 822–827.

[29] M.K. Aroua, S.P.P. Leong, L.Y. Teo, C.Y. Yin, W.M.A.W. Daud, Real-time determination of kinetics of adsorption of lead(II) onto palm shell-based activated carbon using ion selective electrode, Bioresour. Technol. 99 (2008) 5786–5792.

[30] E.-K. Guechi, O. Hamdaoui, Sorption of malachite green from aqueous solution by potato peel: Kinetics and equilibrium modeling using non-linear analysis method, Arabian J. Chem. (in press), doi:10.1016/j.arabjc.2011.05.011.

[31] C.H. Giles, T.H. MacEwan, S.N. Nakhwa, D. Smith, 786. Studies in adsorption. Part XI. A system of classification of solution adsorption isotherms, and its use in diagnosis of adsorption mechanisms and in measurement of specific surface areas of solids, J. Chem. Soc. 111 (1960) 3973–3993.

[32] I. Langmuir, The constitution and fundamental properties of solids and liquids. Part I. Solids, J. Am. Chem. Soc. 38 (1916) 2221–2295.

[33] H. Freundlich, W. Heller, The Adsorption of cis- and trans-Azobenzene, J. Am. Chem. Soc. 61 (1939) 2228–2230.

[34] M.J. Temkin, V. Pyzhev, Kinetics of ammonia synthesis on promoted iron catalysts, Acta Physicochim. URSS 12 (1940) 217–222.

[35] M.M. Dubinin, L.V. Radushkevich, The equation of the characteristic curve of the activated charcoal, Proc. Acad. Sci. USSR Phys. Chem. Sec. 55 (1947) 331–337.

[36] V. Vadivelan, K.V. Kumar, Equilibrium, kinetics, mechanism, and process design for the sorption of methylene blue onto rice husk, J. Colloid Interface Sci. 286 (2005) 90–100.

[37] S. Chowdhury, R. Mishra, P. Saha, P. Kushwaha, Adsorption thermodynamics, kinetics and isosteric heat of adsorption of malachite green onto chemically modified rice husk, Desalination 265 (2011) 159–168.

[38] G. McKay, J.F. Porter, G. Prasad, The removal of dye colors from aqueous solutions by adsorption on low-cost materials, Water Air Soil Pollut. 114 (1999) 423–438.

[39] B.H. Hameed, Evaluation of papaya seeds as a novel non-conventional low cost adsorbent for removal of methylene blue, J. Hazard. Mater. 162 (2009) 939–944.

[40] K.S. Low, C.K. Lee, The removal of cationic dyes using coconut husk as an absorbent, Pertanika 13 (1990) 221–228.

[41] L.S. Oliveira, A.S. Franca, T.M. Alves, S.D.F. Rocha, Evaluation of untreated coffee husks as potential biosorbents for treatment of dye contaminated waters, J. Hazard. Mater. 155 (2008) 507–512.

[42] G. McKay, G. Ramprasad, P. Pratapa Mowli, Equilibrium studies for the adsorption of dyestuffs from aqueous solutions by low-cost materials, Water Air Soil Pollut. 29 (1986) 273–283.

[43] F. Banat, S. Al-Asheh, L. Al-Makhadmeh, Evaluation of the use of raw and activated date pits as potential adsorbents for dye containing waters, Process Biochem. 39 (2003) 193–202.

[44] G. Annadurai, R. Juang, D. Lee, Use of cellulose-based wastes for adsorption of dyes from aqueous solutions, J. Hazard. Mater. 92 (2002) 263–274.

[45] R. Han, Y. Wang, P. Han, J. Shi, J. Yang, Y. Lu, Removal of methylene blue from aqueous solution by chaff in batch mode, J. Hazard. Mater. 137 (2006) 550–557.

[46] K.V. Kumar, Optimum sorption isotherm by linear and non-linear methods for malachite green onto lemon peel, Dyes Pigm. 74 (2007) 595–597.

[47] R. Ahmad, R. Kumar, Adsorption studies of hazardous malachite green onto treated ginger waste, J. Environ. Manage. 91 (2009) 1032–1038.

[48] A. Mittal, L. Krishnan, V.K. Gupta, Removal and recovery of malachite green from wastewater using an agricultural waste material de-oiled soya, Sep. Purif. Technol. 43 (2005) 125–133.

[49] G.H. Sonawane, V.S. Shrivastava, Kinetics of decolourization of malachite green from aqueous medium by maize cob (*Zea maize*): An agricultural solid waste, Desalination 247 (2009) 430–441.

[50] S. Chowdhury, P. Saha, Sea shell powder as a new adsorbent to remove Basic Green 4 (Malachite Green) from aqueous solutions: Equilibrium, kinetic and thermodynamic studies, J. Chem. Eng. 164 (2010) 168–177.

[51] A. Altınışık, E. Gür, Y. Seki, A natural sorbent, *Luffa cylindrica* for the removal of a model basic dye, J. Hazard. Mater. 179 (2010) 658–664.